Egypt. J. Chem. **Vol. 67**, No. 10 pp. 209- 224 (2024)

Egyptian Journal of Chemistry

http://ejchem.journals.ekb.eg/

In vitro anti-diabetic effect and molecular docking study of *Phlomis aurea* components as diabetic enzymes inhibitor

Mayada M. El-Azab[1], Marwa A. Ibrahim[1] , Taha A.I. El-Bassossy[*1] and Fatma A. Ahmed[1]

[1]*Medicinal and Aromatic Plants Department, Desert Research Center, Cairo, Egypt*

Abstract

The aim of this study was to assess the potential of *Phlomis aurea* extracts [hexane (Hex), ethyl acetate (EtOAc) and methanol (MeOH)] on anti-diabetic property using *in vitro* yeast cell model and inhibited α-amylase, α-glucosidase and sucrase activities. Our study focused on the chemical constituents of the most active extract of *P. aurea* plant as anti-diabetic activity and molecular docking investigation of the ligand (bioactive compounds) in the active binding site of target protein (α–glucosidase, α-amylase, and sucrase). EtOAc extract exhibited the most effective extract where, it significantly increased yeast cells capacity to absorb glucose (86.24%) and inhibited α-amylase, α-glucosidase and sucrase activities with IC_{50} values (1.99, 1.22 & 2.1 mg/mL) as compared to the IC_{50} value (2.51, 1.67 & 0.89 mg/mL), of acarbose reference drug, respectively. EtOAc extract containing a large amount of phenolic and flavonoid compounds, as 68 phenolic compounds were identified using LC-MS technique, where chalcone, diosmin, naringenin, rhoifolin, apigenin-7-O-glucoside, chlorogenic acid, luteolin-7-O-glucoside, hesperidin, quinic acid, peonidine-3-O-glucoside chloride, apigenin, acacetin, 7-hydroxy-4-methylcoumarin, cyanidin-3-glucoside, datiscin, were the high concentration of identified phenolic constituents. The majority of these compounds exhibited strong binding affinities to α -amylase, α-glucosidase and sucrase catalysts and showed great *in-silico* results compared with reference inhibitor against target compounds.

Keywords: *Phlomis aurea*, ethyl acetate extract, anti-hyperglycemic, phenolic, flavonoid compounds, molecular docking analysis.

INTRODUCTION

A metabolic disease termed diabetes mellitus is marked by high levels of glucose in blood brought on by abnormalities in the release of insulin, action, or both [1]. In Egypt, it is a relatively common chronic illness that causes significant socioeconomic issues, particularly in cities where an unhealthy lifestyle is prominent. Drugs are widely available, but they come with a long list of adverse effects. Additionally, the drug should be switched out periodically because the body eventually develops tolerance to it [2]. One remedial methodology for diminishing postprandial hyperglycemia in patients with diabetes mellitus is forestalling the assimilation of carbs after food take-up. Just monosaccharaides, like glucose and fructose, can be moved out of the intestinal lumen into the circulatory system. Before being absorbed by the duodenum and upper jejunum, complex starches, oligosaccharides, and disaccharides must be broken down into individual monosaccharides. Enteric enzymes attached to the brush border of intestinal cells, such as pancreatic α-amylase and α-glucosidases, facilitated this digestion [3]. α-Amylase and α-glucosidase are required carbohydrates hydrolyzing enzymes answerable for breaking α, 1-4 bonds in disaccharides and polysaccharides, delivering glucose [4,5,6]. Sucrase is a digestive enzyme that catalyzes the hydrolysis of sucrose to its component monosaccharide, fructose, and glucose. Free glucose is then absorbed by the stomach then released to bloodstream and results in postprandial hyperglycemia. Postprandial hyperglycemia is reduced, and carbohydrate digestion and glucose absorption are slowed by inhibition of sucrase, α-amylase, and α-glucosidase [7]. A few past logical reports have revealed insight into the hindrance of these critical proteins by bioactive compounds from plants [6,8]. The hindrance of these enzymes with diminishing the pace of absorption of sugars so less

*Corresponding author e-mail: tahachemist2008@gmail.com ; (Taha A. I. El-Bassossy).
Receive Date: 13 April 2024, Revise Date: 03 May 2024, Accept Date: 14 May 2024
DOI: 10.21608/ejchem.2024.282603.9587

glucose is ingested that the carbohydrates are not separated into glucose particles. Plants and natural products could represent an excellent source for drugs since they can provide new compounds which cannot be predicted by synthetic chemistry [9]. The genus *Phlomis* has played a significant role in the discovery of natural harmaceuticals. Within the Lamiaceae family, *Phlomis* is a vast genus that has over 100 species spread across the continents of North Africa and Europe [10]. Generally, its flower components are used as a herbal tea to cure digestive issues and to support overall health by guarding the kidney, liver, bone, and cardiovascular system [11]. Certain *Phlomis* species are also used in cooking. *Phlomis* species are referred to as herbal medicines and are utilized ethno-pharmacologically in herbal medicine for the treatment of respiratory tract diseases and wounds on the skin. Some *Phlomis* species are utilized in people medication for their pain relieving and antidiarrheal properties, and for the treatment of ulcers and hemorrhoids. *Phlomis,* pharmacological and biological effects are poorly documented. A few examinations have shown different activities, for example, anti-inflammatory, immuno-suppressive, hostile to mutagenic, anti- nociceptive, antifebrile, free radical scavenging, anti- malarial, and anti- microbial impacts [12].

The primary goal of the current study was to examine the impact of various *P. aurea* plant extracts on glucose uptake by yeast cells and on some carbohydrate hydrolyzing enzymes (α-amylase, α-glucosidase, and sucrase), due to the background information provided and the lack of prior reports regarding *P. aurea* antidiabetic properties. To determine the active compounds in the most potent extract of *P. aurea* plant, a LC-MS technique investigation of the extract was done. Moreover, the *in-silico* binding mode of these compounds in the objective proteins was explained through the docking choice utilizing autodocking via programming.

MATERIALS AND METHODS

Plant material and authentication:

The aerial parts of *P. aurea* were collected in May 2022 from Wadi Alarbaeen in Saint Catherine, Sinai, Egypt (33° 56' 60" East and 28° 33' 5" North). The identification and nomenclature were carried out and approved by Dr. Abdel-Hameed U.K. The voucher specimen was stored as UKA015-20 in the herbarium of the Botany Department, Faculty of Science, Ain Shams University, Cairo, Egypt.

Extraction of plant material

The air-dried powdered of *P. aurea* aerial parts (300 g) were extracted successively by soxhlet apparatus starting with n-hexane, with increasing polarity by EtOAc and finally MeOH for 48 h till exhaustion for each solvent where the temperatures guidelines of extractions were followed by not exceeding 55 ºC to minimize any fragmentation of the chemical components and to maintain the chemical skeleton without changing their structure. Each extract was concentrated under vacuum to yield semisolid extracts (8 g, 2.4 g, 6.2g), respectively. The EtOAc extract most have anti-diabetic activity was subjected to LC-ESI-TOF-MS analysis.

Chemicals Used

The analytical grade chemicals and reagents utilized in this investigation were all purchased from Sigma-Aldrich Co. in the United States. Thermo-Fisher Scientific (Waltham, MA, USA) provided the HPLC grade acetonitrile and methanol needed for LC-MS analysis, while Sigma-Aldrich Co. (USA) supplied the formic acid (98%), ammonium hydroxide, and ammonium formate.

LC-ESI-TOF-MS analysis of ethyl acetate extract

LC-ESI-TOF-MS analysis of the EtOAc were carried out as specified by [13] at the Children's Cancer Hospital in Cairo, Egypt's Proteomics and Metabolomics Research Program. Both positive and negative techniques of injection were used for the sample. The apparatus descriptions, techniques, methods of sample analysis and its identification were described in [14, 15] and software that is open-source [16] was employed for the sample's thorough small-molecule, non-targeting examination. As reference databases, Positive respect (2737 records) or negative respect (1573 records) databases were employed depending on the acquisition technique.

In vitro antidiabetic assays

Glucose uptake in yeast cell

Repeated centrifugation (3,000×g, 5 min) was used to clean Easy Grow Baker's commercial baker's yeast by distilled water until a clear supernatant was obtained. Further, 10% (v/v) suspension was ready with something similar. 1 mL of glucose solution contained extracts of varying concentrations (10-500 mg/mL), and the mixture was incubated at 37°C for 10 minutes. The response was started by adding 100 µL of yeast suspension, vortexed, and incubated at 37°C. After 60 minutes, the tubes were centrifuged (2500×g, 5 min), and the amount of glucose in the supernatant was estimated. Berberine was used as a typical medication. The following formula was used to determine the percentage increase in glucose absorption by yeast cells [17]. Absorbance was estimated at 540 nm and all tests were done in sets of three.

% Increase glucose uptake = Absorbance control-Absorbance sample/ Absorbance control × 100.

α -Amylase inhibition assay

A colorimetric method with 3, 5-dinitrosalicylic acid (DNS) reagent was utilized to measure the α-amylase inhibitory activity [18]. 250 µL of extracts (1-5 mg/mL) with 250 µL of porcine pancreatic α-amylase

enzyme (1 unit) was pre-incubated for 20 min at 37 °C. The response was started by the addition of 250 µL of 1% potato soluble starch followed by incubated for 10 min at 37 ˚C. The response was halted with the addition of 0.5 µL of DNS reagent, brooded in boiling water bath for 10 min, the tubes were cooled, and absorbance was taken at 540 nm, acarbose was viewed as a positive control. The following equation was used to determine the percentage of inhibition.
% Inhibition = Absorbance of control-Absorbance of extract/Absorbance of control × 100.

α -Glucosidase inhibition assay
α-glucosidase inhibitory action was assessed [18] with a few slight modifications. 50 µL of the tested extracts (ranging from 1 to 5 mg/mL) and 240 µL of yeast α-glucosidase enzyme (1 unit/mL) were added to the reaction mixture after it had been pre-incubated for 20 minutes at 37°C. 40 µl of *p*-Nitrophenyl-α-D-glucopyranoside (5 mM) was added to begin the response, and it was then incubated for 10 min before 750 µL of Na_2CO_3 (0.2 M) was added. As a positive control, acarbose was regarded. At 405 nm, absorbance was measured. The level of inhibition was determined.
% Inhibition = Absorbance of control-Absorbance of extract/Absorbance of control × 100.

Sucrase inhibition assay
The methodology of a previous study was slightly modified for the purpose of determining sucrase inhibitory effect [19]. Phosphate Buffer Saline (PBS) was used to prepare sucrase, sucrose, and a variety of sample solutions with varying concentrations (ranging from 1 to 5 mg/ml). The enzyme solution of 10 µl and various concentrations of samples were placed in glass test tubes then incubated at 37°C for ten minutes. After that, 100 µl of 60 mM sucrose was added to the tube and malate buffer (pH 6.0) was used to increase the volume to 200 µl. The tubes were left to incubate once more for thirty minutes at 37°C. Each tube received 200 µl of DNS reagent after the incubation was completed. The response was ended by placing the tubes in boiling water bath for 10 min. A UV-Vis spectrophotometer was used to measure the samples' absorbance at 540 nm. The following formula was used to determine sucrase inhibition:
% Inhibition = Absorbance of control-Absorbance of extract/Absorbance of control × 100.

Molecular docking study
Our Extracted natural products were screened against α-amylase, α-glucosidase, and sucrase enzymes target sites to predict the expected anti-diabetic activity. In the crystal protein structure, the binding sites were made by co-crystallized the ligands with the target proteins (PDB codes: 1b2y, 3w37, and 3lpp). Water molecules were initially removed from the complex. Next, preparation options were used to prepare, correct crystallographic disorders, and empty valence atoms. Utilizing CHARMM force fields, energy consumption of protein structures was reduced. Hence, defining and preparing the pockets for the docking process. Utilizing Chem-Bio Draw Ultra17.0, 2D designs of tried compounds were drawn and saved as SDF files, the saved documents were opened, 3D designs were protonated, and 0.1 RMSD kcal/mole energy was minimized by the MMFF94 force field. Then, the limited designs were ready for docking through the ligand readiness instruments. The docking was completed through the docking option using Autodock vina software. The receptor was held unbending while the ligands were permitted to be adaptable. During the refinement every atom was permitted to deliver ten distinct stances with the proteins. Then docking scores (affinity energy) of the best-fitted postures with the active sites were recorded and 3D orientations were generated by Discovery Studio 2016 visualizer.

Statistical analysis
The mean and standard deviation of three parallel measurements are used to represent the data. IC_{50} values were determined by plotting a percent inhibition versus concentration curve for *in vitro* examines, in which the concentration of sample required for 50% inhibition was determined and expressed as IC_{50} value.

RESULTS AND DISCUSSION

Chemical investigation
The analysis of EtOAc extract using LC-MS/MS in both negative and positive mode of ionization revealed the presence of number of classes including alkaloids, fatty components, steroids, vitamins, hormones, terpenoids, phenolic components (flavonoids and phenolic acids), with a large number of unidentified compounds. In our study, we investigated the chemical constituents of the EtOAc extract of *P. aurea* which exhibited the most potent anti-diabetic activity using LC-Ms-TOF especially phenolic constituents (phenolic acids and flavonoids). The outlined results in table 1 confirmed that, the plant extract had 68 phenolic constituents which were abundant in *P. aurea* extract and represented more than 75 % of total contents, we concerned to discuss them in this study where, most of the flavonoid biochemical components were responsible for biological activity of the plant especially polymethoxy flavones, flavonols and flavonons. All compounds were distinguished by looking at the precise mass determination and the retention time with those of reference standards. The itemized MS data of phenolic parts were recorded in table 1 and they were recognized in light of precise mass determination of precursor ions and their fragment peaks, which were compared with relevant literatures compounds. Out lined data recorded in table 1 showed chalcone (11.52%), diosmin (9.54%), naringenin (6.39%), rhoifolin (5.99%), chlorogenic

acid (5.83%), apigenin-7-O-glucoside (4.13%), luteolin-7-O-glucoside (4.08%), hesperidin (2.74%), quinic acid (2.54%), peonidine-3-O-glucoside chloride (2.53%), apigenin (2.53%), acacetin (2.32%), 7-hydroxy-4-methylcoumarin (2.25%), cyanidin-3-glucoside (1.85%), datiscin (1.55%) were the high concentration of identified phenolic constituents, the literature and our previous studies proved that most of these compounds have anti-inflammatory, anti-diabetic, antimicrobial and anticancer activities [20, 21, 15]. The illustration of mass fragmentation pathways of some high percent compounds were discussed in the following schemes (1: 13) and table 1. Scheme 1 showed proposed Ms/Ms fragmentation of a protonated molecule peak $[M+H]^+$ at m/z 209 which produce a prominent peak at m/z 131, corresponds to the loss of the phenyl group from the A ring. Other important peaks include m/z 105 due to loss of CO from the benzylic cation, m/z 77 (tropylium ion) and m/z 51 (loss of acetylene molecule). The suggested pathways of Ms fragmentation to produce the most stable cation by resonance of the double bond in aromatic system at m/z 105 $[C_8H_8]^+$ and 77 $[C_6H_5]^+$. The obtained data is accordance to those reported by [22] which predicted the chemical structure of chalcone compound. Scheme 2 showed the possible Ms fragmentation of m/z 609.16 protonated carbocation $[M+H]^+$, there are some predicted pathways of fragmentation where, the flavone atom lost one sugar moiety bringing about the section [M+H- rhamnose m.wt 164]$^+$ (m/z 463), the glucose m.wt 180 moiety was additionally lost yielding the aglycone diosmetin $[M+H]^+$ (m/z 301) which presented high stability component with intensity 100% of fragmentation, then there other loss of methyl group of OCH_3 group from the aglycone moiety to give other stable cation by conjugation double bonds in the aromatic system and resonance (m/z 286 $[M+H-CH_3]^+$) followed by sequential loss of small molecules such as C_8O and CH_2O and rearrangement of the compound to give molecule peaks with m/z 177, 147 and 117 with intensity (53, 47 and 41%). These pathways predict the compound identification was agreement with diosmin which reported in [23, 24]. Scheme 3 illustrates the MS fragmentation pathways of naringenin are characterized by the formation of several characteristic fragment ions. The most prominent fragment ions are m/z 273, 153 and 109. The parent peak at m/z 273.08 was corresponding to protonated cation $(M+H)^+$ while, m/z 153 was formed by a retro-Diels-Alder reaction, which involves the cleavage of the C ring followed by elimination of one molecule CO_2 [25]. While in scheme 4, the probable fragmentation of rhoifolin ($C_{27}H_{30}O_{14}$) showed parent ion m/z 579.15 at positive ionization mode $(M+H)^+$, after cleavage of glycosidic bond between aglycone and rutinosidic moiety (glucose and rhamnose bond) showed stable aglycone cation at m/z 271 with molecular formula ($C_{15}H_{10}O_5$) (54% intensity) followed by retro-Diels-Alder reaction and cleavage of C ring to give m/z 147 ($C_6H_{14}O_4$) (80% intensity) finally to give more stable carbocation m/z 73 ($C_3H_5O_2$ 100%) after losing C_3H_6O molecule. Scheme 5 illustrated that the structure of chlorogenic acid ($C_{16}H_{18}O_9$ m/z 355.10 $[M+H]^+$) consist of two phenolic acids (caffeic $C_9H_8O_4$ and quinic acid $C_7H_{12}O_6$), where it can naturally formed by ester bond between caffeic acid and quinic acid with losing H_2O molecule. Due to its structural complexity, it exhibited characteristic fragmentation patterns in mass spectrometry where the fragmentation behavior of chlorogenic acid influenced by the presence of the caffeic acid and the quinic acid moiety, which undergo different fragmentation pathways. At the first, the ester bond between two acids was broken to give stable cation of two acids where dehydrocaffeic acid ion (m/z 179) results from the passing of a water particle (-H_2O) from the caffeic acid moiety while, (m/z 191). This ion formed due to the cleavage of the ester bond between caffeic acid and quinic acid. Then loss of CO_2 from caffeic acid ion (m/z 135), on the other hand, elimination of a water molecule from the quinic acid ion produce (m/z 173 with intensity 100%) followed by elimination small molecule (CO m/z 145) then lose one (H_2O m/z 127) [26, 27]. The previous fragmentation of chlorogenic acid can be considered to be also for D(-) quinic acid as shown in scheme 5 [28]. The mass fragmentation of apigenin-7-O-glucoside illustrated in scheme 6 where the fragmentation pathways mechanisms including glycosidic cleavage, retro-Diels-Alder reactions, and loss of neutral fragments. The primary fragmentation pathway involves the loss of the glucose moiety (162 m/z) from the protonated molecular ion ($[M+H]^+$) of apigenin-7-O-glucoside (m/z 433.11). This cleavage occurs via glycosidic bond cleavage by heterolysis, resulting in the formation of the aglycone apigenin (m/z 271) and a protonated glucose ion (m/z 181). The fragmentation of the C-ring of apigenin can proceed through retro-Diels-Alder reactions, leading to the formation of characteristic fragment ions. These reactions involve the breaking of carbon-carbon bonds and the formation of new cyclic structures. Other pathway of neutral fragments can also be lost from apigenin-7-O-glucoside, contributing to its fragmentation pattern. These include the loss of carbon monoxide (28 m/z) and formaldehyde (30 m/z). Also the fragmentation of apigenin aglycone was discussed in this compound [29, 30]. The fragmentation of luteolin-7-O-glucoside ($C_{21}H_{20}O_{11}$ m/z 447.09) illustrated in the scheme 7 which involved similar pathways of apigenin-7-O-glucoside of cleavage of glycosidic bond to give aglycone moiety, followed by retro-Diels-Alder reactions by breaking of carbon-carbon bonds and the formation of new cyclic structures. Furthermore, hesperidin undergoes various fragmentation pathways during MS fragmentation analysis, primarily involving the cleavage of bonds

within its molecular structure. These pathways can be categorized into various pathways, mainly, loss of the sugar portion: This is the most common fragmentation pathway, resulting from breaking down the glycosidic link in the flavanone aglycone and the rutinose sugar moiety. The resulting fragment ion is the flavanone aglycone, with a mass-to-charge ratio (m/z) of 301, followed elimination of small molecules (CH_3) resulting m/z 286 then (CO) to give stable carbocation at m/z 258. Other pathways probably occurred of hesperidin fragmentation illustrated in the scheme 8 [31]. Scheme 9, the fragmentation of peonidin-3-O-glucoside chloride (PgCl) with a molecular formula of $C_{22}H_{23}O_{11}$+Cl^- undergoes fragmentation to produce several characteristic ions. The major fragmentation pathways for PgCl are summarized as loss of the glucose portion, the most prominent fragmentation pathway for PgCl involves the loss of the glucose portion ($C_6H_{12}O_6$), resulting in the formation of the aglycone ion $[M-G]^+$ at m/z 301. The heterolytic cleavage C-O bond between the aglycone and the glucose moiety can also undergo heterolytic cleavage, leading to the formation of ions at m/z 286 $(M-CH_3]^+$ and 258 $(M-CH_3-CO)^+$. In addition to, the aglycone itself can also undergo fragmentation by retro-Diels-Alder reactions (rDA), producing cation ion at m/z 151 followed with rearrangement and enlarged the six ring to tropylium cation ring at m/z 107, which are characteristic of the flavonoid C ring. Scheme 10 showed possible pathways of acacetin fragmentation involved elimination of small molecule such as CH_3 group and CO molecule followed rDA reaction of heterolytic cleavage of the C-O bond of furan ring to give two stable radicals by ring resonance (124, 117 m/z). The proposed interpretation of mass fragmentation of 7-hydroxy-4-methylcoumarin ($C_{10}H_8O_3$ m/z 177.06) was discussed in scheme 11 which involved cleavage of C-O, C-C bonds and eliminate the small molecules as CO, CH_2, CH_3 throw the fragmentation process followed by the rearrangement of the bonds and atoms to get more stable cation at m/z 149 of $C_9H_8O_2$ intensity 100%, $C_7H_5O_2$ m/z 121 with intensity 70 %, $C_7H_7^+$ with intensity 60 % m/z 91, $C_6H_5^+$ m/z 77 with intensity 52 [23]. Otherwise, the fragmentation of cyanidin-3-O-glucoside elucidated in scheme 12 involved heterolytic breaking down the glycosidic link that connects the glucose moiety and the aglycone (cyanidin). Two ions are produced as a result: the glycosyl ion (m/z 162) and the protonated aglycone ion (m/z 287). The heterolytic cleavage of the glycosidic bond is a common fragmentation pathway for glycosides where, the glycosidic bond is a relatively weak bond, and it can be easily broken in the MS instrument. The second stage of fragmentation involves the fragmentation of the protonated aglycone ion. The major fragmentation pathways were cross-ring cleavage, this involves the cleavage of the C_2-C_3 bond, resulting in the formation of two ions: m/z 137 represented the C_2-C_3 fragment and m/z 151 corresponding to the C_3-C_4 fragment. The cross-ring cleavage is a common fragmentation pathway for anthocyanins where, the C_2-C_3 bond is relatively weak, and it can be easily broken in the MS instrument followed by sequential loss of neutral molecules such as CO, O atom and other pathways can involve H_2O, from the protonated aglycone ion. The neutral molecules that are lost are typically small and stable, and they can be easily eliminated from the molecule in the MS instrument. The C_3-C_4 fragment is a stabilized zwitterion due to the presence of two oxygen atoms and their corresponding protonation and deprotonation. While The C_2-C_3 fragment is a simple cation with a carbonyl group [23]. On the other side the datiscin mass fragmentation proposed pathways interpreted in scheme 13 which showed parent ion m/z 286 after cleavage of the glycosidic bonds which presented more stable cation with molecular formula ($C_{15}H_{10}O_6$), this ion undergo for various fragmentations such as loss of H_2O) to give m/z 268 where, this fragmentation occurs due to the labile nature of the hydroxyl group (-OH), which easily loses a proton to form a carbocation. The carbocation then rearranges and loses a water molecule to form a more stable ion. Others due to the heterolytic cleavage of the A-ring to give m/z 201 and 84. Also can undergo to sequence elimination of neutral compounds as CO then CO_2 to give finally molecular formula $C_{13}H_{10}O_3$ m/z 214.

Table 1: List of the identified phenolic compounds from EtOAc extract of *P. aurea* by LC–ESI-TOF–MS in both positive and negative modes with their retention times, molecular formula and mass spectral data

	Proposed compounds	RT.	m/z	%	Adduct	Formula	Ms Fragmentation
1	Thymol	1.01	151.03	0.01	$[M+H]^+$	$C_{10}H_{14}O$	151, 135, 68
2	Kaempferol-3-O-alpha-l-rhamnoside	1.09	431.12	0.09	$[M-H]^-$	$C_{21}H_{20}O_{10}$	431, 362, 294
3	D-(-)-Quinic acid	1.09	191.05	2.54	$[M-H]^-$	$C_7H_{12}O_6$	191, 173, 127, 93
4	Isorhamnetin-3-O-rutinoside	1.13	623.18	0.01	$[M-H]^-$	$C_{28}H_{32}O_{16}$	623, 461, 191, 161
5	Salicylic acid	1.21	137.02	0.05	$[M-H]^-$	$C_7H_6O_3$	137, 93
6	P-Hydroxybenzoic acid	1.40	139.06	0.09	$[M+H]^+$	$C_7H_6O_3$	139, 95, 79
7	Baicalein-7-O-glucuronide	4.09	445.14	0.07	$[M-H]^-$	$C_{21}H_{18}O_{11}$	445, 359, 269, 240
8	7-Hydroxy-4-methylcoumarin	4.11	177.06	2.25	$[M+H]^+$	$C_{10}H_8O_3$	177, 149, 134, 121, 91, 77
9	Chalcone	4.14	209.08	11.52	$[M+H]^+$	$C_{15}H_{12}O$	209, 131, 105, 77, 53
10	Myricitrin	4.43	463.11	0.07	$[M-H]^-$	$C_{21}H_{20}O_{12}$	463, 417, 394, 300 208., 194., 150
11	Chlorogenic acid	4.77	355.10	5.83	$[M+H]^+$	$C_{16}H_{18}O_9$	355, 191, 179, 173, 135, 145, 127
12	4-Methoxycinnamic acid	4.94	179.07	0.13	$[M+H]^+$	$C_{10}H_{10}O_3$	179, 161, 79
13	Okanin-4'-O-glucoside	5.10	449.11	0.03	$[M-H]^-$	$C_{21}H_{22}O_{11}$	449, 241
14	Luteolin-3', 7-di-O-glucoside	5.27	611.16	0.03	$[M+H]^+$	$C_{27}H_{30}O_{16}$	611, 563, 473, 455, 243
15	3,4-Dimethoxycinnamic acid	5.45	209.08	0.92	$[M+H]^+$	$C_{11}H_{12}O_4$	209, 191, 159, 149, 131, 103, 77
16	Isorhamnetin-3-O-glucoside	5.47	477.10	0.04	$[M-H]^-$	$C_{22}H_{22}O_{12}$	477, 445, 341
17	Hesperetin	5.94	301.12	0.12	$[M-H]^-$	$C_{16}H_{14}O_6$	301, 177, 151, 134
18	Procyanidin b2	5.95	579.17	0.4	$[M+H]^+$	$C_{30}H_{26}O_{12}$	579, 562, 547, 440, 427, 410, 121
19	Daidzein-8-c-glucoside	6.00	417.18	0.09	$[M+H]^+$	$C_{21}H_{20}O_9$	417, 399, 167, 133
20	4'-Hydroxyisoflavone-7-O-glucoside	6.06	415.16	0.69	$[M-H]^-$	$C_{21}H_{20}O_9$	415, 278, 149
21	Apigenin 8-C-glucoside	6.44	431.10	0.07	$[M-H]^-$	$C_{21}H_{20}O_{10}$	431, 311, 228
22	Cyanidin-3-O-(2"-O-beta-xylopyranosyl-beta-glucopyranoside)	6.47	581.15	0.31	$[M]^+$	$C_{26}H_{29}O_{15}$	581, 449, 287
23	Quercetin-3-d-xyloside	6.63	433.12	0.1	$[M-H]^-$	$C_{20}H_{18}O_{11}$	433, 417, 303, 285, 133
24	Acacetin-7-O-rutinoside	6.76	593.19	0.03	$[M+H]^+$	$C_{28}H_{32}O_{14}$	593, 447, 285, 270, 242
25	Isookanin-7-glucoside	6.81	449.11	0.21	$[M-H]^-$	$C_{21}H_{22}O_{11}$	449, 287, 151, 135
26	Cyanidin-3-O-glucoside	6.84	449.10	1.85	$[M]^+$	$C_{21}H_{21}O_{11}$	449, 287, 151, 137, 109, 77
27	Luteolin	6.88	287.05	0.05	$[M+H]^+$	$C_{15}H_{10}O_6$	287, 227, 153
28	Luteolin-7-O-glucoside	6.93	447.09	4.08	$[M-H]^-$	$C_{21}H_{20}O_{11}$	447, 287,151, 133, 107
29	Hyperoside	6.99	465.15	0.3	$[M+H]^+$	$C_{21}H_{20}O_{12}$	465, 303, 271, 255, 243, 150
30	Myricetin	7.05	319.12	0.02	$[M+H]^+$	$C_{15}H_{10}O_8$	319, 149, 137, 109, 98
31	Petunidin-3-O-beta-glucopyranoside	7.07	479.12	0.39	$[M]^+$	$C_{22}H_{23}O_{12}$	479, 317, 302, 271, 163
32	Glycyrrhizate	7.18	821.25	0.03	$[M-H]^-$	$C_{42}H_{62}O_{16}$	821, 755, 645, 352, 289
33	Ononin	7.42	431.17	0.13	$[M+H]^+$	$C_{22}H_{22}O_9$	431, 267, 252, 223
34	Apigenin-7-O-glucoside	7.63	433.11	4.13	$[M+H]^+$	$C_{21}H_{20}O_{10}$	433, 271, 243 153, 109
35	Naringenin	7.63	273.08	6.39	$[M+H]^+$	$C_{15}H_{12}O_5$	273, 153, 109
36	Peonidine-3-O-glucoside chloride	7.82	463.12	2.53	$[M]^+$	$C_{22}H_{23}O_{11}$	463, 301, 286, 258
37	Malvidin-3-O-glucoside chloride	7.98	493.13	0.85	$[M]^+$	$C_{23}H_{25}O_{12}$	493, 331, 316
38	Neohesperidin dihydrochalcone	8.06	611.14	0.08	$[M-H]^-$	$C_{28}H_{36}O_{15}$	611, 567, 303, 293, 197, 137
39	Naringenin-7-O-glucoside	8.24	435.17	0.03	$[M+H]^+$	$C_{21}H_{22}O_{10}$	435, 417, 387, 273, 233, 181, 167
40	Kaempferol-3-glucuronide	8.31	463.09	0.16	$[M+H]^+$	$C_{21}H_{18}O_{12}$	463, 430, 301, 287
41	Kaempferol-7-neohesperidoside	8.48	593.18	0.06	$[M-H]^-$	$C_{27}H_{30}O_{15}$	593, 473, 353, 287
42	Apigenin-6-c-glucoside-7-O-glucoside	8.49	595.19	0.04	$[M+H]^+$	$C_{27}H_{30}O_{15}$	595, 447, 327
43	Sabinene	8.55	137.06	0.26	$[M+H]^+$	$C_{10}H_{16}$	137, 122, 94, 66
44	Hesperetin-7-O-neohesperidoside	8.60	609.19	0.03	$[M-H]^-$	$C_{28}H_{34}O_{15}$	609, 449, 304, 164, 151
45	Quercetin-3,4'-O-di-beta-glucopyranoside	8.72	625.16	0.07	$[M-H]^-$	$C_{27}H_{30}O_{17}$	625, 579, 503, 299
46	Eriodictyol-7-O-neohesperidoside	8.82	595.14	0.2	$[M-H]^-$	$C_{27}H_{32}O_{15}$	595, 577, 473, 269, 145
47	Kaempferol-3-O-alpha-l-arabinoside	9.13	419.16	0.05	$[M+H]^+$	$C_{20}H_{18}O_{10}$	419, 373, 287, 243
48	Peonidin-3,5-O-di-beta-glucopyranoside	9.23	625.20	0.08	$[M]^+$	$C_{28}H_{33}O_{16}$	625, 301, 287
49	Kaempferol-3-O-(6-p-coumaroyl)-glucoside	9.29	593.13	0.41	$[M-H]^-$	$C_{30}H_{26}O_{13}$	593, 285, 255, 227
50	Rhoifolin	9.95	579.15	5.99	$[M+H]^+$	$C_{27}H_{30}O_{14}$	579, 271, 147, 73
51	3, 5, 7-Trihydroxy-4'-methoxyflavone	10.01	301.07	0.07	$[M+H]^+$	$C_{16}H_{12}O_6$	301, 284, 256
52	Datiscin	10.15	593.13	1.55	$[M-H]^-$	$C_{27}H_{30}O_{15}$	593, 286, 268, 252, 214, 84
53	Cyanidin-3-O-rutinoside	10.19	595.15	0.42	$[M]^+$	$C_{27}H_{31}O_{15}$	595, 449, 287
54	Apigenin	10.90	271.06	2.53	$[M+H]^+$	$C_{15}H_{10}O_5$	271, 179, 152, 117
55	Hesperidin	11.14	609.16	2.74	$[M-H]^-$	$C_{28}H_{34}O_{15}$	609, 301, 286, 258, 151, 107
56	Diosmin	11.15	609.16	9.54	$[M+H]^+$	$C_{28}H_{32}O_{15}$	609, 463, 301, 286, 177, 147, 117
57	Quercitrin	11.19	447.25	0.04	$[M-H]^-$	$C_{21}H_{20}O_{11}$	447, 300, 271, 255, 243, 150
58	Rosmarinic acid	11.81	359.08	0.07	$[M-H]^-$	$C_{18}H_{16}O_8$	359, 329, 200, 161, 134
59	Genistein	12.14	271.23	0.04	$[M+H]^+$	$C_{15}H_{10}O_5$	271, 260, 197
60	Quercetin	12.29	303.08	0.39	$[M+H]^+$	$C_{15}H_{10}O_7$	303, 167, 163, 145, 135
61	Caffeic acid	12.75	181.13	0.49	$[M+H]^+$	$C_9H_8O_4$	181, 163, 139, 135, 121, 107, 91
62	Quercetin-4'-glucoside	12.77	465.12	0.03	$[M+H]^+$	$C_{21}H_{20}O_{12}$	465, 303, 150
63	4',5,7-Trihydroxyflavonol	13.81	272	0.49	$[M-H]^-$	$C_{15}H_{10}O_6$	272, 168
64	Acacetin	14.04	285.07	2.32	$[M+H]^+$	$C_{16}H_{12}O_5$	285, 270, 242, 124, 117
65	3'-Methoxy-4',5,7-trihydroxyflavonol	14.09	315.09	0.91	$[M-H]^-$	$C_{16}H_{12}O_7$	315, 302, 385, 168
66	3' 4' 5 7-Tetrahydroxyflavanone	14.32	289.18	0.02	$[M+H]^+$	$C_{15}H_{12}O_6$	289, 163, 153, 145, 135, 117
67	(+-)-Taxifolin	18.68	305.15	0.04	$[M+H]^+$	$C_{15}H_{12}O_7$	305, 287, 273, 259, 194, 153
68	3 3' 4' 5-Tetrahydroxy-7 methoxyflavone	25.89	317.11	0.15	$[M+H]^+$	$C_{16}H_{12}O_7$	317, 225, 113

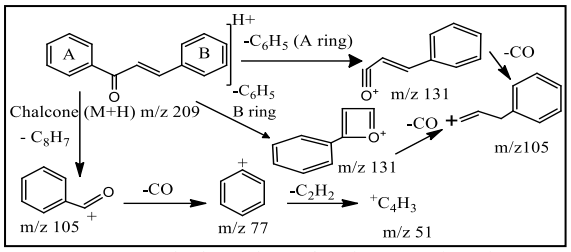

Scheme (1): Proposed scheme for Ms/Ms fragmentation of chalcone

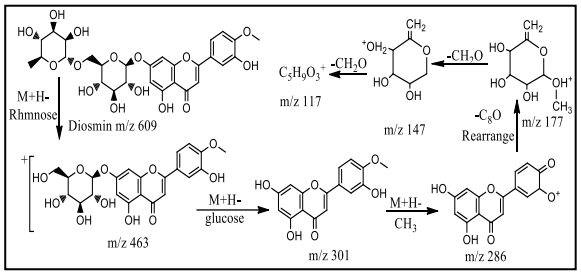

Scheme (2): Proposed pathways for Ms/Ms fragmentation of diosmin

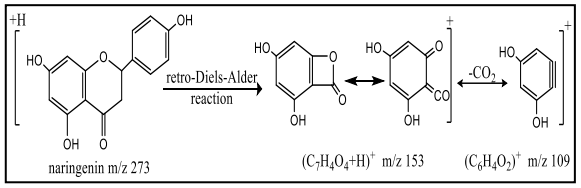

Scheme (3): Suggested pathway for Ms/Ms fragmentation of naringenin

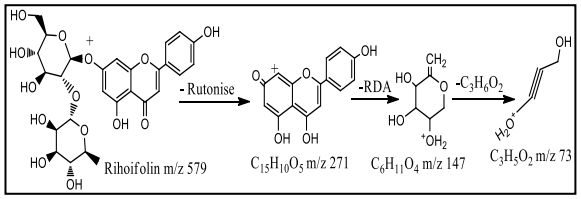

Scheme (4): Suggested pathway for Ms/Ms fragmentation of riholifolin

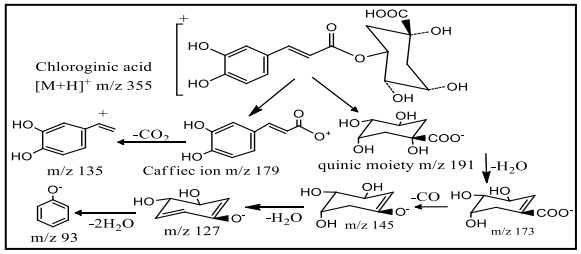

Scheme (5): Suggested Pathway for Ms/Ms fragmentation of chlorogenic acid and quinic acid

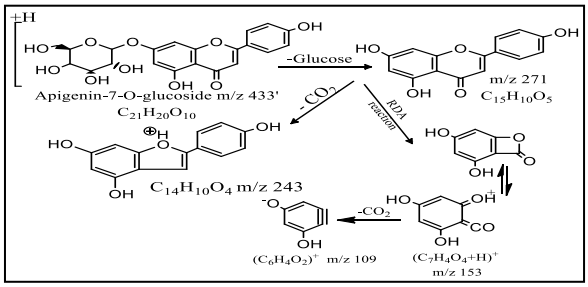

Scheme (6): Probable pathways for Ms/Ms fragmentation apigenin-7-O-glucoside

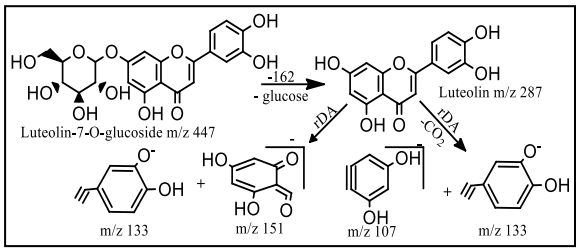

Scheme (7): Probable pathways for Ms/Ms fragmentation lutolien-7-O-glucoside

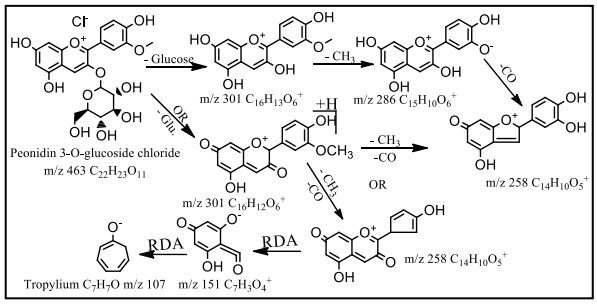

Scheme (8): Proposed pathways for Ms/Ms fragmentation of hesperidin

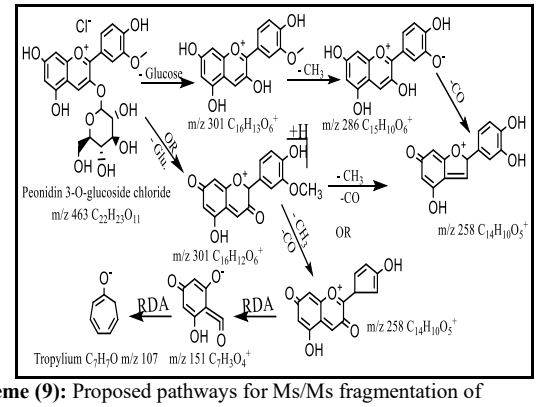

Scheme (9): Proposed pathways for Ms/Ms fragmentation of peonidine-3-O-glucoside chloride

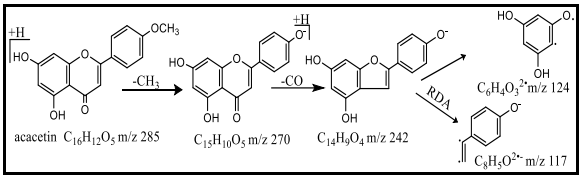

Scheme (10): Proposed interpretation pathways for Ms/Ms fragmentation of acacetin

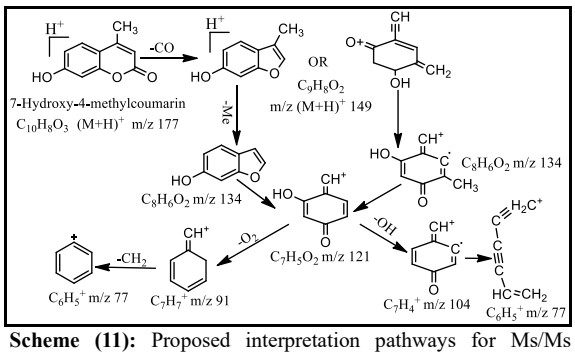

Scheme (11): Proposed interpretation pathways for Ms/Ms fragmentation of 7-hydroxy -4-methylcoumarin

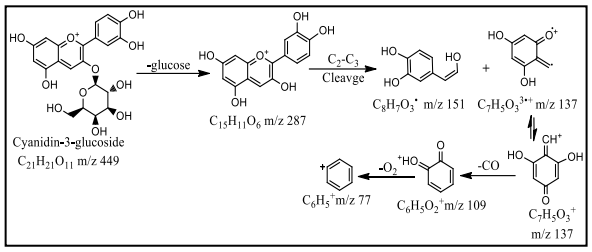

Scheme (12): Proposed interpretation pathways for Ms/Ms fragmentation of cyanidin-3-O-glucoside

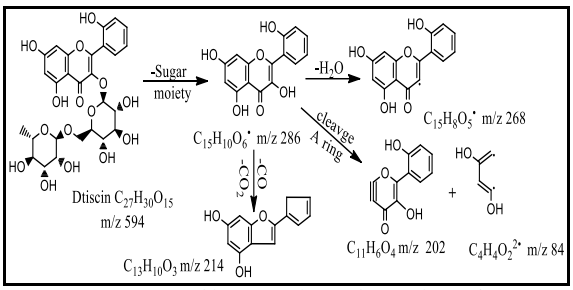

Scheme (13): Proposed interpretation pathways for Ms/Ms fragmentation of datiscin

Effect of *Phlomis aurea* extracts on glucose uptake by yeast cell

The impact of *P. aurea* extracts on glucose transport across yeast cell membrane was assessed in an *in vitro* framework that incorporates yeast cells suspended in a glucose solution at 5 mM in the presence/nonappearance of the extract. The amount of glucose that remains in the medium after a certain amount of time is a sign of how much glucose the yeast cells consume. Yeast cells' ability to absorb glucose increased in a dose-dependent manner when *P. aurea* extracts were added to the medium. This increase was correlated exactly with the concentration of extract explained in fig. (1). The % of glucose uptake was (94.53, 86.24, 63.32 & 59.08) by berberine, EtOAc, MeOH & Hex, respectively at 500 µg/mL. The results revealed that EtOAc extract of *P. aurea* induced the highest glucose absorption by yeast cells. The mechanism of glucose transport across the yeast cell membrane has been getting consideration as an *in vitro* technique for hypoglycemic impact of different compounds and medicinal plants [19]. Numerous factors, such as the quantity and digestion of glucose inside yeast cells, may influence the transport of glucose across membranes in yeast. The intracellular concentration of glucose will drop, and the cell's absorption of glucose will increase if the majority of the inside glucose is converted into other metabolites [32]. Like this, greater glucose metabolism and easier diffusion may be involved in the transfer of glucose moves across the yeast cell membrane when EtOAc extract is present. Generally, tannins and flavonoids may play an important role in this diffusion [33, 34], and in accordance with our results of LC-ESI-TOF-MS examination revealed that among the principal constituents present in EtOAc extract are flavonoids.

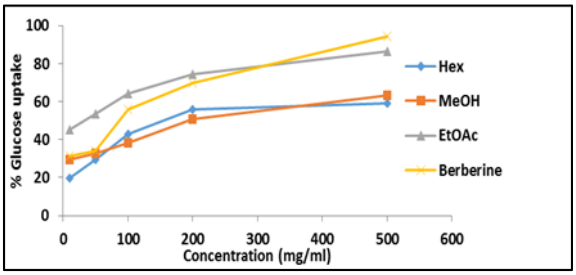

Fig. (1): Effect of berberine and *P. aurea* extracts on glucose uptake by yeast cells.

Effect of *Phlomis aurea* extracts on α-amylase, α-glucosidase, and sucrase activities

The effect of *P. aurea* extracts on α-amylase, α-glucosidase, and sucrase activities is presented in figs (2-4) & table (2). Hex, EtOAc & MeOH extracts inhibited α-amylase, α-glucosidase, and sucrase activities in a dose dependent manner. This inhibitory activity was communicated with regards to IC_{50}. The IC_{50} value of Hex, EtOAc & MeOH extracts was 10.65, 1.99 & 2.20 on α-amylase and 3.06, 1.22 & 2.19 on α-glucosidase and 3.12, 2.10 & 3.34 mg/mL on sucrase, respectively. The IC_{50} value of reference drug, acarbose was (2.51, 1.67 & 0.89 mg/mL) on α-amylase, α-glucosidase & sucrase activities, respectively. A lower IC_{50} value demonstrates higher inhibition, and that intends that, EtOAc extract have the most elevated inhibitory action on α-amylase, α-glucosidase and sucrase activities [35] mentioned that the hindrance of α-amylase, α-glucosidase and sucrase is including the most valuable strategies to lessen postprandial hyperglycemia in T2DM patients. It has been demonstrated that natural products are one of the most important sources for DM medication discovery. Various plants have been demonstrated to go about as antihyperglycemic specialists alone or as complementary treatments with other antidiabetic agents. In the current study, EtOAc extract exhibited considerable enzyme inhibition potentials. Consequently, we analyzed EtOAc extract using LC–MS/MS in both negative and positive mode of ionization which revealed the presence of number of compounds classes including (flavonoids and phenolic acids), there is evidence that flavonoid compounds have an anti-diabetic effect due to the ability to inhibit the α-amylase and α-glucosidase enzymes. The inhibition occurs when hydrogen bonds are formed between the hydroxyl groups on flavonoids and the catalytic residues on enzyme. Consequently, starch digestion and postprandial glycemia are reduced due to the synergy between the enzyme and flavonoids [36].

Table (2): IC_{50} values of acarbose and *P. aurea* extracts based on α-amylase, α-glucosidase and sucrase inhibition assays

Samples	IC_{50} value (mg/ml)		
	α-Amylase inhibition	α-Glucosidase inhibition	Sucrase inhibition
Hex	10.65	3.06	3.12
EtOAc	1.99	1.22	2.10
MeOH	2.20	2.19	3.34
Acarbose	2.51	1.67	0.89

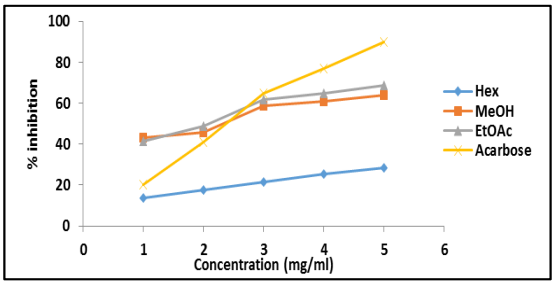

Fig. (2): Effect of acarbose and *P. aurea* extracts on α-amylase activity

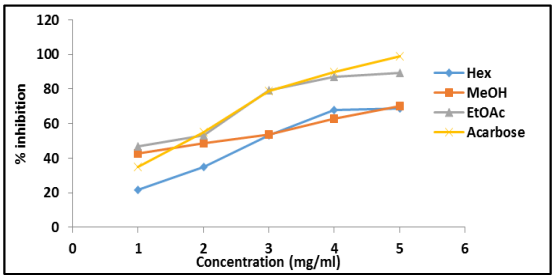

Fig. (3): Effect of acarbose and *P. aurea* extracts on α-glucosidase.

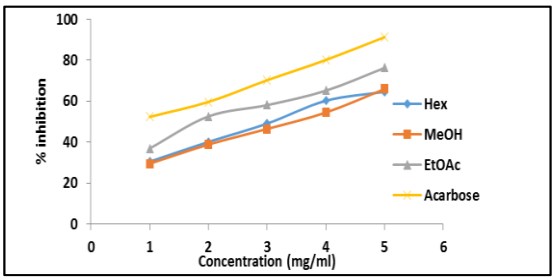

Fig. (4): Effect of acarbose and *P. aurea* extracts on sucrase activity

Molecular Docking Study

Acarbose is considered an effective anti-diabetic agent by acting as a competitive reversible inhibitor of sucrase, α-glucosidase, and α-amylase enzymes. The inhibition of these enzymes causes the gut to absorb glucose more slowly and reduces the postprandial rise in insulin and glucose in the blood. Acarbose, was used as (reference inhibitor) against target enzymes, it exhibited binding energies of -9.50, -9.25, and -8.50 kcal/mol against α-amylase, α-glucosidase and sucrase enzymes, respectively. The binding pocket of α-amylase enzyme contains Asp300, Glu233, Asp197, His305, Lys200, Gln63, Tyr151, and Gly306 as main interacting amino acids, α-glucosidase enzyme contains Asp232, Asp469, His626, Asp357, Arg552, Trp432, and Trp329, and sucrase enzyme contains His629, Arg555, Asp371, Asp472, Lys509, Trp435, and 355 as critical amino acids, Out of 15 docked ligands tested in this study, the ones with the best S-scores and interactions with these active amino acids were selected and given in Table 3. Which acarbose formed a hydrophobic π-interaction with Leu165, and three ionic interactions with Asp197, Asp300, and Glu233, additionally interacting with Glu240, Lys200, His201, Trp59, Gln63, Thr163, Gly306, Arg195, Glu233, Asp197, His299, Asp300, His101, and His305 by seventeen hydrogen bonds, against α-amylase enzyme (Fig 5a). While the interaction between acarbose and α-glucosidase enzyme showed one hydrophobic π-interaction with Met470, and four ionic interactions with Asp469, Asp568, and Asp232, additionally interacting with Asp357, His626, Asp568, Arg552, Asp232, Ala234, and Asn237 by thirteen hydrogen bonds (Fig 5b). Additionally, the binding with sucrase enzyme exhibited twelve hydrogen bonds with Gln232, Trp435, Asp355, His629, Asp571, Arg555, Asp231, and Lys509, moreover, formed two hydrophobic π-interaction with Phe604, Trp327, and three ionic interactions with Asp231, Asp472, and Asp371(Fig 5c).

The co-crystalized ligand complexed with sucrase enzyme as competitive inhibitor, showed ten hydrogen bonds and supported by four ionic attractive interaction with Asp355, His629, Asp571, Arg55, Asp231, Lys509, and Asp472, respectively, additionally, formed two π-interactions with Trp435, and Trp327 (Fig 5 d).

α-Amylase inhibition

When diosmin bound to the α-amylase enzyme, its binding energy was -8.90 kcal/mol. It's formed six hydrophobic π-interactions with Trp59, Asp300, Ala307, Ile235, and Leu237. Additionally, diosmin interacted with Glu240, Gln63, Glu233, and Lys200 by six hydrogen bonds with distances range 1.84 to 3.06 Å (Fig 6a). The mechanism of binding of chlorogenic acid showed a -8.66 kcal/mol binding energy against the α-amylase enzyme. Three hydrophobic π-interactions were created with His201, Leu162, and Ile235, moreover, interacted with Lys200, His305, and Gln63 by four hydrogen bonds with lengths range 1.98 to 2.86 Å (Fig 6b). Apigenin-7-O-glucoside showed a binding energy of -7.43 kcal/mol against the α-amylase enzyme. Six hydrophobic π-interactions were created with Trp59, Asp300, Asp197, and Tyr62. Additionally, apigenin-7-O-glucoside interacted with Ile235, His201, Asp197, and His299 by four hydrogen bonds separated by lengths of 2.21, 2.35, 2.04, and 2.40 Å (Fig 6c). The binding mode of luteolin-7-O-glucoside demonstrated a binding energy of -7.63 kcal/ mol against α-amylase enzyme. It formed three π-interactions that are hydrophobic with Asp300, and Trp59. Furthermore, luteolin-7-O-glucoside interacted with Gln63, Lys200,

His201, and Glu233 by four hydrogen bonds with length range 2.01 to 2.47 Å (Fig 6d). The binding mode of hesperidin exhibited a binding energy of -8.34 kcal/ mol against the α-amylase enzyme. Hesperidin formed five hydrophobic π-interactions with Trp59, Tyr151, Leu237, and Leu162. Moreover, interacted with Glu240, Gly306, Glu233, Tyr62, and Gln63 by six hydrogen bonds with distances range 1.97 to 2.10 Å (Fig 6e). Cyanidin-3-glucoside showed a binding energy of -7.14 kcal/ mol against α-amylase enzyme. It formed two hydrophobic π-interactions with Tro59, and Asp300. Also, cyanidin-3-glucoside formed four hydrogen bonds with Gly306, Glu233, and Asp197 with distances of 2.12, 2.22, 1.92 and 1.95 Å (Fig 6f). The binding mode of peonidine-3-O-glucoside chloride exhibited a binding energy of -7.79 kcal/ mol against α-amylase enzyme. peonidine-3-O-glucoside chloride formed three hydrophobic π-interactions with Trp59 and His305 moreover, interacted with Trp59, Gln63, Asp197, and Glu233 by five hydrogen bonds that range in distance from 1.92 to 2.55 Å (Fig 6g).

α-Glucosidase inhibition

Link mode diosmin exhibited a binding power of -9.43 kcal/ mol against α-glucosidase enzyme destination site. diosmin created a single hydrophobic π-interactions with Leu628 and four hydrogen links with Arg578, Ala228, Glu629, and Ser626 with distance ranges of 1.89 to 2.56 Å (Fig 7a). The binding mode of chlorogenic acid demonstrated a binding power of -9.70 kcal/mol against the α-glucosidase enzyme destination site. Chlorogenic acid formed four hydrophobic π-interactions with Phe476, Asp232, Trp329,Trp432 and one attractive interaction with Arg552, moreover, interacted with Lys506, Phe476, Asp357, Trp432, Arg552, and Asp568 eight hydrogen bonds are formed with distances variety of 1.76 to 3.00 Å (Fig 7b). Apigenin-7-O-glucoside a binding energy of -7.89 kcal/mol against the α-glucosidase enzyme destination site. Five hydrophobic π-interactions were generated with Asp568, Met470, Ala234, Ala628, and Ala602. Additionally, apigenin-7-O-glucoside interacted with Asp357, His626, Asp568, Asp232, and Glu603 by five hydrogen bonds with distance of 1.87, 2.03, 2.57, 2.00 and 2.53 Å (Fig 7c). The binding energy of luteolin-7-O-glucoside against the intended target site of the α-glucosidase enzyme was -8.90 kcal/mol. It formed four hydrophobic π-interactions with Ala602, Ala234, Met470, and Asp568. Additionally, luteolin-7-O-glucoside interacted with Glu603, His626, Asp568, Asp357, Asp469, Trp432, and Asp232 by seven hydrogen links that vary in length from 1.97 to 2.67 Å (Fig 7d). When hesperidin bound to the target site of the α-glucosidase enzyme, the binding energy was -9.95 kcal/mol. Hesperidin formed four hydrophobic π-interactions with Met470, Ala234, Asp568, and Ala602, moreover, interacted with Asp232, Trp432, Asp469, Asp357, Asp568, Arg552, Asp630, and Glu603 by ten hydrogen bonds with distances range 1.93, 3.07 Å (Fig 7e). cyanidin-3-glucoside showed a binding energy of -8.01 kcal/ mol against the α-glucosidase enzyme objective site. It exhibited five hydrophobic π-interactions with Trp432, Ile358, Ile396 and Lys 506. Additionally, cyanidin-3-glucoside interacted with Lys506, Asp568, Asp357, His626, and Arg552 by seven hydrogen links that vary in length from 1.92 to 2.98 Å (Fig 7f).

Sucrase inhibition

When diosmin bound to the objective site of the sucrase enzyme, the binding energy was -9.05 kcal/mol. which formed seven hydrophobic π-interactions with Phe479, Lys509, His629, TRp568, Phe604, and Trp470. Additionally, formed six hydrogen bonds with His629, Asp355, Asp472, Asp571, and Lyas509 with distances range of 1.76 to 2.29 Å (Fig 8a). The binding energy of rhoifolin against the objective site of the sucrase enzyme was -7.73 kcal/mol. Rhoifolin showed five interactions of hydrophobic π-type with Ile211, Leu340, Val219, and Ala230, moreover, interacted with Asp290, Lys213, Lys335, Asp351, Ser280 and Lys232 by seven hydrogen links that vary in length from 1.82 to 2.76 Å (Fig 8b). Apigenin-7-O-glucoside demonstrated a -7.75 kcal/mol binding energy against the target region of the sucrase enzyme. It was formed four interactions of hydrophobic π-type with Asp231, Lys509, and Phe479. Additionally, apigenin-7-O-glucoside interacted with Asp355, His629, Asp571, and Arg555 by six hydrogen bonds ranging in distance from 1.95 to 2.57 Å (Fig 8c).

The binding energy of luteolin-7-O-glucoside against the target region of the sucrase enzyme was -8.92 kcal/mol. Four interactions of hydrophobic π-type were formed with Asp571, Leu233, and Lys509. Additionally, luteolin-7-O-glucoside interacted with Arg230, Asp231, Lys509, Gln232, His629, Asp355 and Trp435 by nine hydrogen bonds ranging in distance 2.07 to 2.82 Å (Fig 8d). When datiscin bound to the target site of the sucrase enzyme, its binding energy was -8.30 kcal/mol. Datiscin formed six hydrophobic π-interactions with Leu233, Phe479, Trp435, Ile356, and Trp327, moreover, it was found to interact with Asp355, His629, Asp571, Arg555, and Lys509 by fifteen hydrogen bonds with distances range 1.79 to 2.92 Å (Fig 8e). Diosmin is present in the extract. It has been found to act as a potential inhibitor of α-amylase and α- glucosidase enzymes [37]. Additionally, chlorogenic acid, that also exists between the compounds were identified in EtOAc extract has qualities that may be beneficial to health, such as anti-inflammatory, antioxidant, and anti-diabetic effects [38]. Some reports suggested that chalcone could inhibit α-amylase and α-glucosidase [39].

Table (3): The free energies that bind of tested compounds against α-amylase enzyme, α-glucosidase enzyme, and sucrase according to docking results

Targets screened	Tested compounds	RMSD value (Å)	Docking (Affinity) score (kcal/mol)	Interactions H.B	Interactions π-interaction
α-Amylase enzyme	Diosmin	1.28	-8.90	6	6
	Chlorogenic acid	1.74	-8.66	4	3
	Apigenin-7-O-glucoside	0.97	-7.43	4	6
	Luteolin-7-O-glucoside	1.33	-7.63	4	3
	Hesperidin	1.43	-8.34	6	5
	Cyanidin-3-glucoside	1.94	-7.14	4	2
	Peonidine-3-O-glucoside chloride	1.32	-7.79	5	3
	Acarbose	1.07	-9.50	17	1
α-Glucosidase enzyme	Diosmin	0.95	-9.43	7	5
	Chlorogenic acid	1.23	-9.70	8	4
	Apigenin-7-O-glucoside	1.23	-7.89	5	5
	Luteolin-7-O-glucoside	0.97	-8.90	7	4
	Hesperidin	1.32	-9.95	10	4
	Cyanidin-3-glucoside	1.72	-8.01	7	5
	Acarbose	0.76	-9.25	13	1
Sucrase enzyme	Diosmin	1.29	-9.05	6	7
	Rhoifolin	1.76	-7.73	4	5
	Apigenin-7-O-glucoside	1.08	-7.75	6	4
	Luteolin-7-O-glucoside	1.37	-8.92	9	4
	Datiscin	1.20	-8.30	5	6
	Acarbose	1.36	-8.50	12	2
	Co-crystalized ligand	1.07	-8.10	10	2

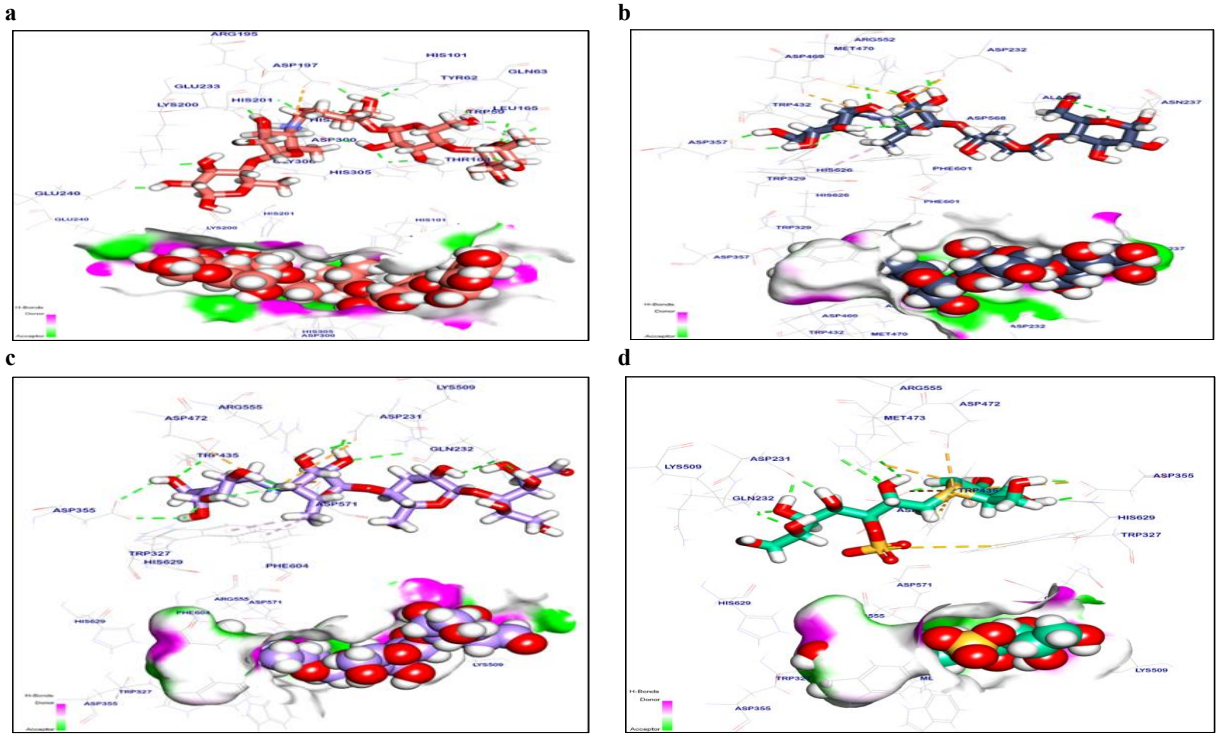

Fig. (5): 3D and surface mapping of acarbose against a: α-amylase, b: α-glucosidase, c: sucrase & d: the co-crystalized ligand complexed with sucrase enzyme

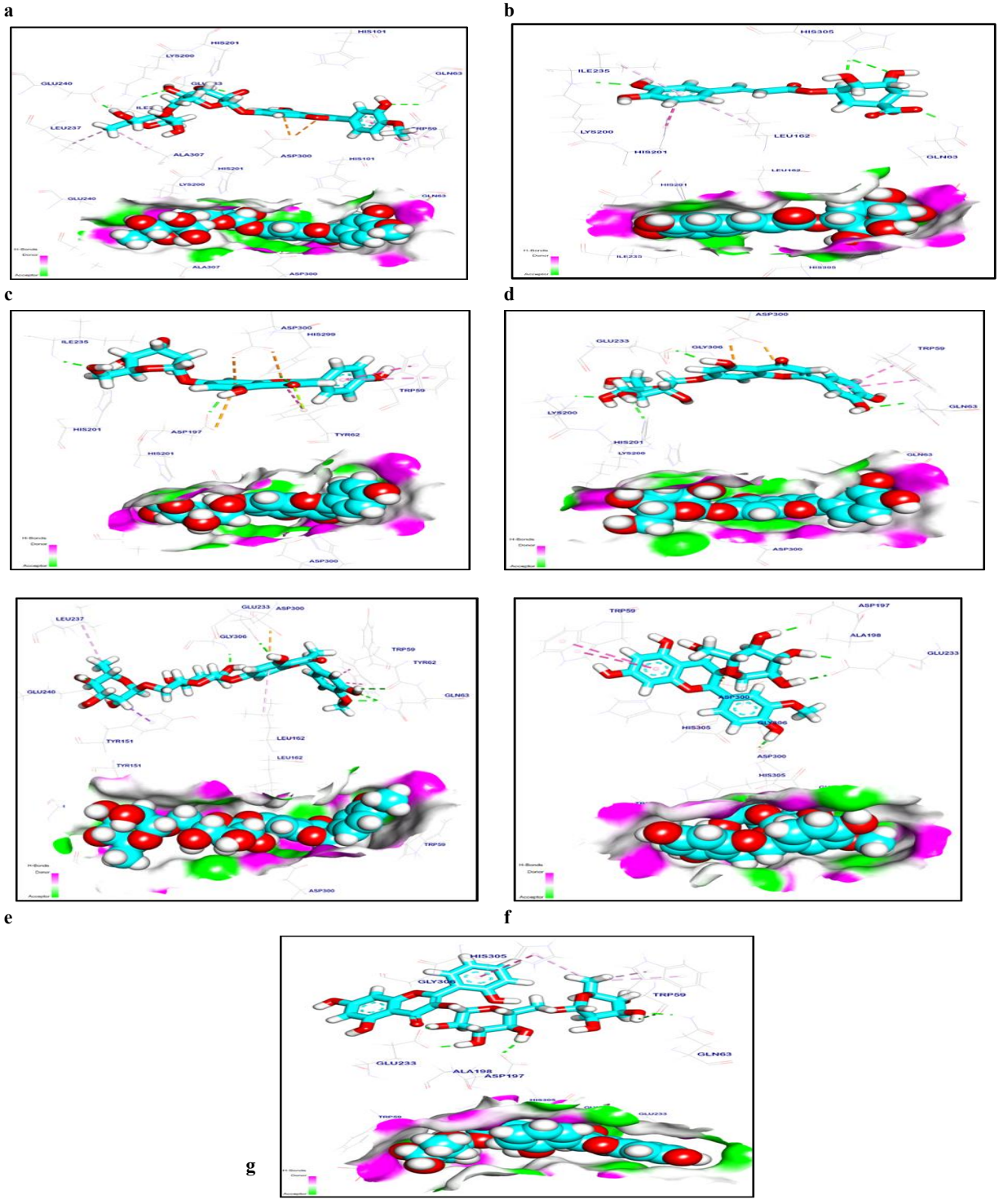

Fig. (6): 3D and surface mapping of **a:** diosmin, **b:** chlorogenic acid, **c:** apigenin-7-O-glucoside, **d:** luteolin-7-O-glucoside, **e:** hesperidin, **f:** cyanidin-3-glucoside & **g:** peonidine-3-O-glucoside chloride against α-amylase enzyme.

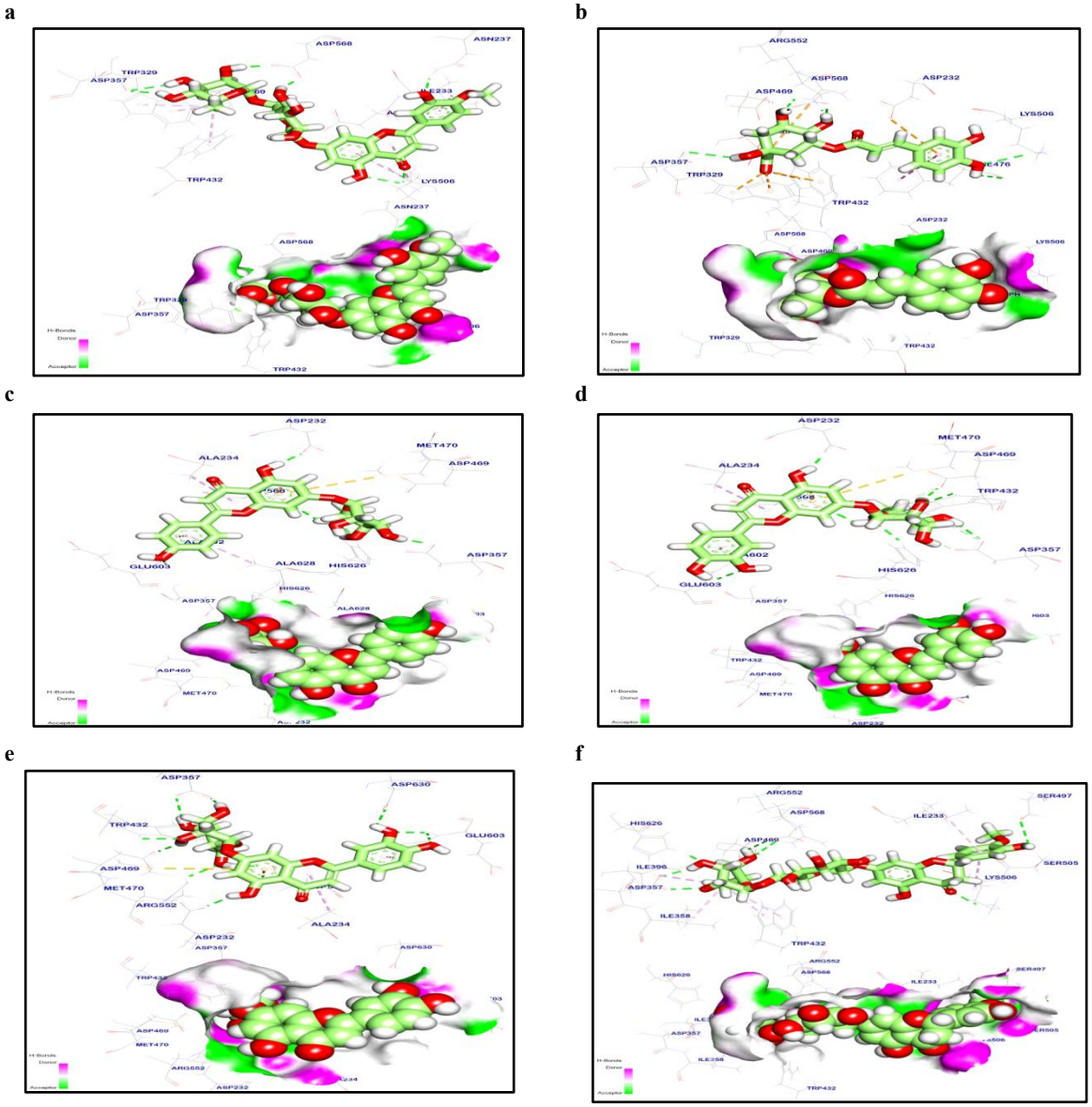

Fig. (7): 3D and surface mapping of **a:** diosmin, **b:** chlorogenic acid, **c:** apigenin-7-O-glucoside, **d:** luteolin-7-O-glucoside, **e:** hesperidin & **f:** cyanidin-3-glucoside against α-glucosidase enzyme.

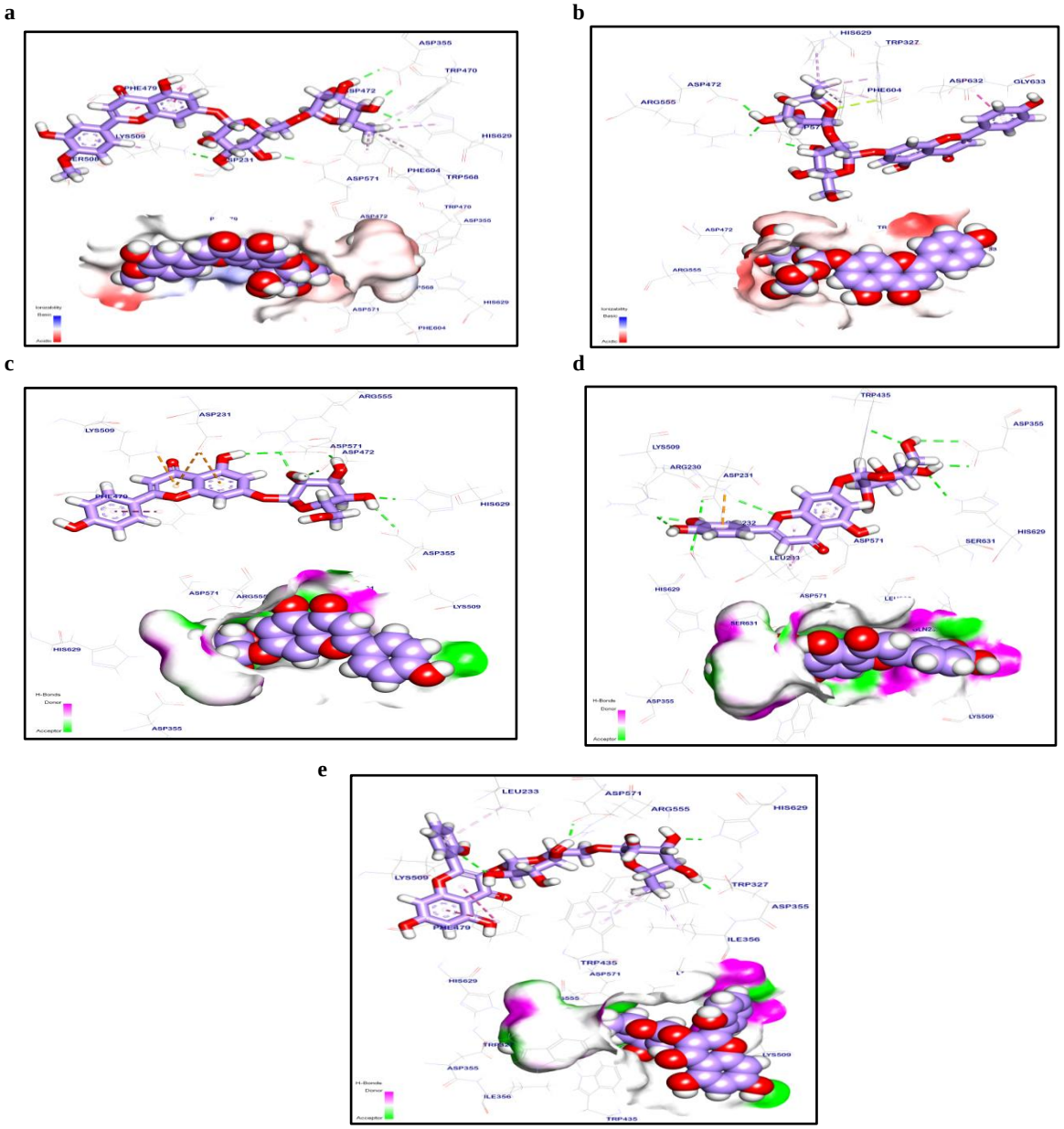

Fig. (8): 3D and surface mapping of **a:** diosmin, **b:** rhoifolin, **c:** apigenin-7-O-glucoside, **d:** luteolin-7-O-glucoside & **e:** datiscin against sucrase enzyme.

Conclusion

The identification of enzyme inhibitors that inhibit pathways contributing to the metabolic process is one of the most important steps in the discovery of new sources of antidiabetic drugs. In the development of a diabetic cure, such inhibitors could work synergistically with natural products. The present study approved that ethyl acetate fraction of *Phlomis aurea* advertised highly significant antihyperglycemic activity among all extracts in vitro anti-diabetic activity. So diabetes and its complications can be treated effectively with this alternative approach.

References

1- Akkati S., Sam K.G., Tungha G. Emergence of promising therapies in diabetes mellitus. *J. Clin. Pharmacol*., 51, 796–804 (2011).

2- Sena C.M., Bento C.F., Pereira P., Marques F., Seiça R. Diabetes mellitus: New challenges and innovative therapies. In: New Strategies to Advance Pre/Diabetes Care: Integrative Approach by PPPM. Netherlands: Springer, p. 29-87(2013).

3- Mohamed E.A.H., Siddiqui M.J.A., Ang L.F., Sadikun A., Chan S.H., Tan S.C., Mohd Z.A., Yam M.F. Potent α-glucosidase and α-amylase inhibitory activities of standardized 50% ethanolic extracts and sinensetin from *Orthosiphon stamineus* Benth as anti-diabetic mechanism *BMC*

Complementary and Alternative Medicine, **12**, 176 (2012).

4- Rolfes S.R., Pinna K., Whitney E. Understanding normal and clinical nutrition; Cengage Learning Inc.: Belmont, CA, USA, (2008).

5- Bhutkar M.A., Bhise SB. *In vitro* assay of alpha amylase inhibitory activity of some indigenous plants. *Int. J. Chem. Sci*., **10**, 457–462 (2012).

6- Carene M.N., Picot A., Subratty H., Mahomoodally F.M. Inhibitory potential of five traditionally used native antidiabetic medicinal plants on α-amylase, α-glucosidase, glucose entrapment, and amylolysis kinetics *in vitro*. *Adv. Pharmacol. Sci*., 1-7 (2014).

7- David S.H., Bell M.B., Type 2 diabetes mellitus: what is the optimal treatment regimen? *The American Journal of Medicine*, **116**, 23–29 (2004).

8- Sembiring N.E., Elya B., Sauriasari R. Phytochemical screening, total flavonoid and total phenolic content and antioxidant activity of different parts of *Caesalpinia bonduc* (L.) Roxb. *Pharm. J*., **10**, 123–127 (2018).

9- Uddin N., Hasan M.R., Hossain M.M., Sarker A., Hasan A.N., Islam A.M., Chowdhury M.M.H., Rana MS. *In vitro* α-amylase inhibitory activity and *in vivo* hypoglycemic effect of methanol extract of *Citrus macroptera* Montr. fruit. *Asian Pac J Trop Biomed*, **4**, 473-479 (2014).

10- Kim J.S. Compositions for inducing secretion of insulin-like growth factor-1.US6, 984, 405 B1. (2006).

11- Amor I.L.-B., Boubaker J., Sgaier M.B., Skandrani I., Bhouri W., Neffati A., Kilani S., Bouhlel I., Ghedira K., Chekir-Ghedira L. Phytochemistry and biological activities of Phlomis species (Review). Journal of Ethnopharmacology, 125 (2): 183-202 (2009).

12- Sarkhail P., Monsef-Esfehani H.R., Amin G., Surmaghi M.H.S., Shafiee A. Phytochemical study of *Phlomis olivieri* Benth. and *Phlomis persica* Boiss. *DARU*, **14**, 115-121 (2006).

13- Mohammed H.A., Khan R.A., Abdel-Hafez A.A., Abdel-Aziz M., Ahmed E., Enany S., Mahgoub S., Al-Rugaie O., Alsharidah M., Aly M.S.A., Mehany A.B.M., Hegazy M.M. Phytochemical profiling, *in vitro* and in silico anti-Microbial and anti-cancer activity evaluations and staph GyraseB and h-TOP-IIβ Receptor-Docking Studies of Major Constituents of *Zygophyllum coccineum* L. aqueous-ethanolic extract and its subsequent fractions: An Approach to validate traditional phytomedicinal knowledge. *Molecules*, **26,** 577-598 (2021).

14- Mohammed H.A., Abdel-Aziz M.M., Hegazy M.M. Anti-oral pathogens of *Tecoma stans* (L.) and *Cassia javanica* (L.) flower volatile oils in comparison with chlorhexidine in accordance with their folk medicinal uses. *Medicina*, **55**, 301-311 (2019).

15- El-Bassossy T.A.I, Abdelgawad AA M, El-Azab, M.M. Induction of apoptosis and cell cycle arrest by ethyl acetate extract of *Salsola kali* and flavonoid constituents analysis. *J. Biologically Act. Prod. Nat*., **13**, 390 – 409 (2023).

16- Tsugawa H., Cajka T., Kind T., Ma Y., Higgins B., Ikeda K., Kanazawa M., Vander Gheynst J., Fiehn O., Arita M. MS-DIAL: data-independent MS/MS deconvolution for comprehensive meta-bolome analysis. *Nature Methods*, **12**, 523-526 (2015).

17- Harish M., Ahmed F., Urooj A. *In vitro* hypoglycemic effects of *Butea monosperma* Lam. leaves and bark. *Food Sci. Technol*, **51**, 308–314 (2011).

18- Thengya S., Thiantongin P., Sontimuang C., Ovatlarnporn C., Puttarak P. α-glucosidase and α-amylase inhibitory activities of medicinal plants in Thai antidiabetic recipes and bioactive compounds from *Vitex glabrata* R.Br. stem bark. *J. Herb. Med*., **19**, 1–8 (2019).

19- Ahmed F., Chandra J.N.N and Timmaiah N. An *in vitro* study on the inhibitory activities of Eugenia jambolana seeds against carbohydrate hydrolyzing enzymes. *Journal of Young Pharmacists* **1**, 317-321 (2009).

20- El-Bassossy T.A. Chemical constituents and biological efficacy evaluation of *Traganum Nudatum* Aerial Parts. *Egypt. J. Chem*, **65**, 521 – 530 (2022).

21- Abdelgawad AA M., El-Bassossy, T.A.I., Ahmed F.A. A review on phytochemical, pharmacological and ethnopharmacological aspects of genus *Trichodesma*. *Indian Journal of Natural Products and Resources*, **12**, 333-347 (2021).

22- Tai Y., Pei S., Wan J., Cao X., Pan Y. Fragmentation study of protonated chalcones by atmospheric pressure chemical ionization and tandem mass spectrometry. *Rapid Commun. Mass Spectrom*, 20, 994–1000 (2006).

23- Allen F., Pon A., Greiner R., Wishart, D. Computational prediction of electron ionization mass spectra to assist in GC/MS compound identification. *Anal Chem*, **88**, 7689-7697 (2016).

24- Chen X., Xu L., Guo S., Wang Z., Jiang L., Wang F., Zhang J., Liu B. Profiling and comparison of the metabolites of diosmetin and diosmin in rat urine, plasma and feces using UHPLC-LTQ-Orbitrap MSn. *Journal of Chromatography*, **1124**, 58-71 (2019).

25- Xu F., Liu Y., Zhang Z., Yang C., Yuan T. Quasi-MS^n identification of flavanone 7-glycoside isomers in Da Chengqi Tang by high performance liquid chromatography-tandem mass spectrometry. *Chinese Medicine*, **4**, 15-30 (2009).

26- Clifford M.N., Herbert K.J. Structural analysis of chlorogenic acids by electrospray ionization

tandem mass spectrometry. *Rapid Communications in Mass Spectrometry* **12**, 1293-1299 (1998).

27- Xue M., Shi H., Zhang J., Liu Q., Guan J., Zhang J.Y., Ma Q. Stability and degradation of caffeoylquinic acids under different storage conditions studied by high-performance liquid chromatography with photo diode array detection and high-performance liquid chromatography with electrospray ionization collision-induced dissociation tandem mass spectrometry. *Molecules*, **21**, 948-960 (2016).

28- Ben Said R., Hamed A.I., Mahalel U.A., Al-Ayed A.S., Kowalczyk M., Moldoch J., Oleszek W., Stochmal A. Tentative characterization of polyphenolic compounds in the male flowers of *Phoenix dactylifera* by liquid chromatography coupled with mass spectrometry and DFT. *Int. J. Mol. Sci*., **18**, 512-523 (2017).

29- Ahmed S., Bhuiyan T. R. Identification of apigenin-7-O-glucoside in *Chrysanthemum morifolium* Ramat. using liquid chromatography-mass spectrometry. *Journal of Natural Medicines*, **66**, 672-676 (2012).

30- Chen Y., Li W. Characterization of flavonoids and their glycosides in *Chrysanthemum morifolium* Ramat. by liquid chromatography-mass spectrometry. *Journal of Food Science and Technology*, **48**, 438-443 (2013).

31- Xu F., Liu Y., Zhang Z., Yang C., Tian Y. Quasi-MS^n identification of flavanone 7-glycoside isomers in Da Chengqi Tang by high performance liquid chromatography-tandem mass spectrometry. *Chinese Medicine*, **17**, 65-79 (2022).

32- Rehman G., Hamayun M., Iqbal A., Ul Islam S., Arshad S., Zaman K., Ahmad A., Shehzad A., Hussain A., Lee I. *In vitro* antidiabetic effects and antioxidant potential of *Cassia nemophila* pods. *BioMed Res. Int*., **2018**, 1-7 (2018).

33- Abu T., Rex-Ogbuku E., Idibiye K. A review: secondary metabolites of *Uvaria chamae* P. Beauv. (Annonaceae) and their biological activities. *Int J Agric Environ Food Sci*, **2**, 177-185 (2018).

34- Hasan M.M, Ahmed Q.U., Mat S.Z., Tunna, TS. Animal models and natural products to investigate *in vivo* and *in vitro* antidiabetic activity. *Biomed Pharmacother*, **101**, 833-841. (2018).

35- Ríos J.L., Francini F., Schinella G.R. Natural products for the treatment of type 2 diabetes mellitus. *Planta Medica*, **81**, 975-994 (2015).

36- Lo Piparo E., Scheib H., Frei N., Williamson G., Grigorov M., and Chou C.J., Flavonoids for controlling starch digestion: Structural requirements for inhibiting human α-amylase, *J. Med. Chem*., **51**, 3555-3561 (2008).

37- Dubey K., Dubey R., Gupta R., Gupta A. Exploration of diosmin to control diabetes and its complications-an *in vitro* and in silico approach. *Current Computer-Aided Drug Design* **17**, 307-313 (2021).

38- Farah A., Donfack P. Chlorogenic acids: occurrence, absorption, metabolism, and health effects. *Phytochemistry Reviews* **15,** 179-198 (2016).

39- Muller C.J., Joubert E, de Beer D., Sanderson M., Malherbe C.J., Fey S.J., Louw J. Acute assessment of an aspalathin-enriched green rooibos (Aspalathus linearis) extract with hypoglycemic potential. *Phytomedicine*, **20**, 32–39 (2012).